Interaction Between Concrete Cylinders and Shape-Memory Wires in the Achievement of Active Confinement

Jean-François Destrebecq and Xavier Balandraud

Abbreviations

A	austenite phase
M	martensite phase
M_i	martensite i-variant
As	austenite start transformation temperature
Af	austenite finish transformation temperature
Ms	martensite start transformation temperature
Mf	martensite finish transformation temperature
SMA(s)	shape memory alloy(s)
Ni-Ti	nickel-titanium

1 Introduction

The mechanical behaviour of structural concrete is governed by a process of damage which results from the progress of macro or microcracks in the loaded material [1]. The damaging process can be delayed by applying a uni- or multiaxial compression in order to counterbalance local tensile stresses in the material. This can be achieved by means of passive or active reinforcement, external or internal to the concrete component.

Shape memory alloys (SMAs) are known as smart materials due to their peculiar thermomechanical properties, like the pseudoelasticity and the memory effect [2]. These properties take their origin from an austenite-to-martensite phase transition occurring when stress or temperature changes. In particular, SMAs have the ability to "freeze" the deformation in the martensitic state, then to recover their initial shape in the austenitic state.

J.-F. Destrebecq (✉)
Clermont Université, Université Blaise Pascal, EA 3867, Laboratoire de Mécanique et Ingénieries, BP 10448, F-63000, Clermont-Ferrand, France
e-mail: J-Francois.Destrebecq@univ-bpclermont.fr

A. Öchsner et al. (eds.), *Materials with Complex Behaviour*, Advanced Structured Materials 6, DOI 10.1007/978-3-642-12667-3_2, © Springer-Verlag Berlin Heidelberg 2010

Several reported experiments confirmed the feasibility of creating stresses in concrete components using SMA wires as external or embedded active reinforcement [3–5]. Also, recovery forces resulting from the activation of shape memory effect in SMA rods were used to reduce crack opening in a damaged structure [6]. In all cases, the prestressing was achieved by thermal activation of the shape memory effect in the SMAs. Difficulties of achieving permanent prestressing in the concrete specimens were reported, due to unwanted stress loss upon cooling down of the SMA wires [3]. According to Motavalli et al. [7], the loss is most likely caused by improper choice of the SMA transformation temperatures. Another potential reason is the stress induced austenite-to-martensite phase transition of the SMA [8].

Recently reported experiments showed that SMAs could be used to create confinement stresses in concrete cylinders in order to improve their performances in uniaxial compression. Choi et al. [9] used austenitic and martensitic SMA wires as external active reinforcement. The existence of a confinement effect was estimated indirectly by looking at the concrete behaviour during crush tests. Cylinders wrapped with prestrained martensitic wires showed an increase in their ductility and ultimate compressive strength. On the contrary, cylinders wrapped with austenitic wires at ambient temperature showed a ductility increase without increase in the ultimate strength. The authors concluded in the existence of confinement stresses due to the shape memory effect in the martensitic wires. This conclusion agreed with experimental results previously reported by Krstulovic-Opara and Thiedeman [10] who observed a substantial increase in the ultimate compressive strength of plain concrete cylinders wrapped with SMA wires.

Attempts were done of estimating the progressive stressing of small-scale SMA/concrete specimens caused by the shape recovery process in the SMA [11, 12]. When the shape memory effect was activated by the heating of the specimen, the prestressing effects were usually estimated by comparing strain measurements in the SMA/concrete specimen with strain measurements in a plain concrete companion specimen. By means of this method, compressive prestressing up to 6 MPa has been estimated in mortar samples reinforced with SMA short fibres [12].

The aim of the present work is to investigate the process of confinement of concrete cylinders combined with wrapped SMA wires used as external active reinforcement. The objective is to get a precise description of the mechanisms involved in the development of the confinement stresses due to the thermal activation of the shape memory effect in the SMA. For this purpose, preliminary tests are carried out in order to precisely determine thermomechanical properties of the SMA wire used in the study. The experimental procedure consists in wrapping SMA wires in different martensitic states around a series of concrete cylinders. The circumferential strains in the cylinders are monitored during the thermal activation of the memory effect in the SMA in order to estimate the confinement stress state induced in the concrete by the martensite-to-austenite transformation of the SMA. The transformation temperatures have been chosen in order to highlight the interaction between temperature and recovery stress in the SMA during the transformation process, leading in some cases to partial stress loss due to austenite-to-martensite phase transition of the SMA. The value of the prestrain of the martensitic wire is a key point in the resulting amplitude of the shape memory effect. Having in mind that the wrapping of the wire on the cylinder induces additional strains and stresses in the wire, valuable information is expected from the tests about the influence of the wire curvature on the effective confinement effect.

2 Creating Forces with SMA

Depending on the thermomechanical loading, a given SMA can exhibit different mechanical behaviours. The present section briefly describes the physical phenomena which explain how a SMA component may be used to create large forces taking advantage of the shape memory effect.

The macroscopic properties of SMAs take their origin from a solid-solid phase transition mechanism occurring when stress or temperature changes [2]. The parent phase is called *austenite* (referred to as A below). It has a bold-centered-cubic structure in all known SMAs. The product phase is called *martensite* (referred to as M below). It exhibits different types of structures which mainly depend on the composition. Due to the symmetry breaking involved in the transformation, the martensite phase exhibits multiple *variants* (referred to as M_i below), which correspond to the same crystal with different orientations in space with respect to the parent phase. The atom displacements involved in a transformation $A \rightarrow M_i$ lead to a so-called transformation strain. When the different variants of martensite exist in equal proportion, the macroscopic strain is nearly equal to zero, and the martensite is said to be “self-accommodated” [13].

Figure 1a, b present the phase diagram indicating the material state as a function of temperature and stress. The material can be either purely austenite, or purely martensite (with various proportions of martensite variants), or a mixture of austenite and martensite. Let us describe the evolution of the material state as a function of the thermomechanical loading.

Starting from austenite, the martensite phase can be obtained by decreasing the temperature or by increasing the stress. Figure 1a shows the two lines in the temperature-stress plane which correspond to the beginning and the end of the transformation $A \rightarrow M$:

- The temperature at which the transformation $A \rightarrow M$ starts by cooling is named Ms. The Mf value is the temperature at which the transformation $A \rightarrow M$ finishes. At zero stress, a self-accommodated martensite is obtained, leading to no change in the specimen shape between the austenite state and the martensite state.
- Martensite appears also when stress increases at a given temperature. In this case, the martensite obtained is not self-accommodated. As a result, large strains are obtained.

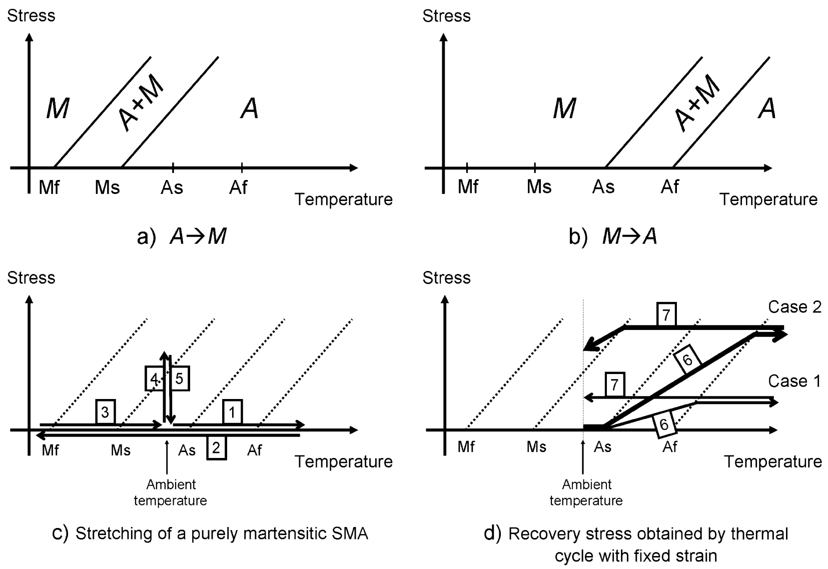

Fig. 1 (**a**) and (**b**) Phase diagrams in the temperature-stress plane. (**c**) and (**d**) Thermomechanical loading steps to create forces in a SMA specimen

Starting now from the martensite phase, changes in the material state can be obtained by increasing the temperature or by stretching the specimen (see Fig. 1b):

– A martensitic specimen returns to austenite state by increasing the temperature. At zero stress, the temperature at which the transformation $M\rightarrow A$ starts is named As. The Af value is the temperature at which the transformation $M\rightarrow A$ finishes.
– The stretching of a purely martensitic specimen at a given temperature leads to a change in its proportions of the martensite variants. The martensite is said to be "reoriented" and the deformation is preserved upon unloading. As a result, different shapes of a given martensitic specimen can be obtained at zero stress.

For Ni-Ti (nickel-titanium) SMAs, it is possible to have Ms < As as shown in Fig. 1 [2]. Let us describe now the capability of creating forces with a Ni-Ti specimen in the case of an ambient temperature between Ms and As. Fig. 1c, d illustrate the thermomechanical loading.

First stage: the objective is to stretch a purely martensitic specimen in order to create a residual strain (prestrain). The following procedure enables to precisely define the level of martensite reorientation (see Fig. 1c):

– step 1: increase the temperature to a value higher than Af in order to obtain a purely austenite specimen.
– step 2: decrease the temperature to a value lower than Mf in order to obtain a purely self-accommodated martensite specimen.

– step 3: return to ambient temperature. The specimen keeps its self-accommodated martensite state (since the ambient temperature is lower than As). No change has occurred in the specimen shape since step 1.
– step 4: apply a mechanical load. The martensite is then reoriented. The shape of the specimen is modified during this loading.
– step 5: return to zero stress. The martensite keeps its reorientation level reached at the end of the previous step. The actual shape of the specimen is different from the initial shape, due to the prestrain caused by the martensite reorientation.

Second stage: the objective is to create active forces at ambient temperature. Starting from step 5, the following procedure is applied (see Fig. 1d):

– step 6: increase the temperature in order to return an austenite state while the strain is fixed. The return to austenite leads to stresses, as the specimen would like to recover its initial shape [14]. Indeed, the free-stress state of the austenite corresponds to a strain equal to zero. As the strain is kept constant to a non-zero value, stresses are created in the specimen. Note that the higher the imposed prestrain obtained by reorientation, the higher the stress obtained.
– step 7: return to ambient temperature. Two cases must be distinguished:

- Case 1: during the temperature decrease, no martensite is created. The corresponding final point in the temperature-stress plane is on the right-hand side of the transformation starting line $A \rightarrow M$ (line including the Ms point). As a consequence, the stress obtained at the end of step 6 is retained at the end of the procedure.
- Case 2: during the temperature decrease, the corresponding point in the temperature-stress plane crosses the transformation starting line $A \rightarrow M$, which means that martensite is created. As a consequence, a decrease in stress is expected because the material optimizes the proportions of martensite variants to relax the stresses in the specimen.

It can be noted that the classic effect of thermal expansion has not been included in this presentation for the sake of simplicity. The next section describes the experimental set-up to perform such a phenomenon with SMA wires wrapped around concrete cylinders.

3 Experimental Set-Up

3.1 Materials

A nickel-titanium ($Ni_{50.8}$-$Ti_{49.2}$, at.%) wire 1 mm in diameter was used in the present study. The choice was motivated by the performance of this type of SMA regarding memory effects. The transformation temperatures were chosen in order to have the austenite-start temperature at about 23°C. The effective transformation temperatures were found as follows:

– martensite to austenite : As = 23°C and Af = 28°C,
– austenite to martensite: Ms = –10°C and Mf = –25°C.

It can be noted that Ms < 20°C < As. This constraint is specially required for the present application involving an ambient temperature at about 20°C. This was achieved by the supplier thanks to a specific thermal treatment.

A series of concrete cylinders were prepared for the tests, 74.4 mm in diameter and 180 mm in height. The moulds were precisely cut from a polyvinyl chloride (PVC) plastic pipe, such that their inside surface was smooth and they were all very similar in geometry. The concrete mix was designed, aiming at a compressive strength about 25 MPa at 28 days. The proportions used for the concrete preparation were as follows (in kg/m^3): gravel 1039.2, sand 782.7, cement 324.5, and water 176.1. Owing to the size of the samples, the maximum size of the coarse aggregate (gravel) was limited to 12.5 mm.

For every cylinder, two pairs of metallic thread inserts were fixed inside the mould before cast, in such a way to have them embedded in the concrete after hardening (see Fig. 2). For each pair, the two inserts were positioned diametrically opposite to each other at a distance of 20 mm from the nearest cylinder end (top and bottom). The inserts were aimed at fixing the SMA wire ends on the cylinder without damaging the concrete.

After cast, the cylinders were kept in the moulds and sealed with plastic foils in order to avoid moisture loss. Foils and moulds were removed after 28 days of hardening. Then the cylinders were kept in ambient in-door atmosphere until testing.

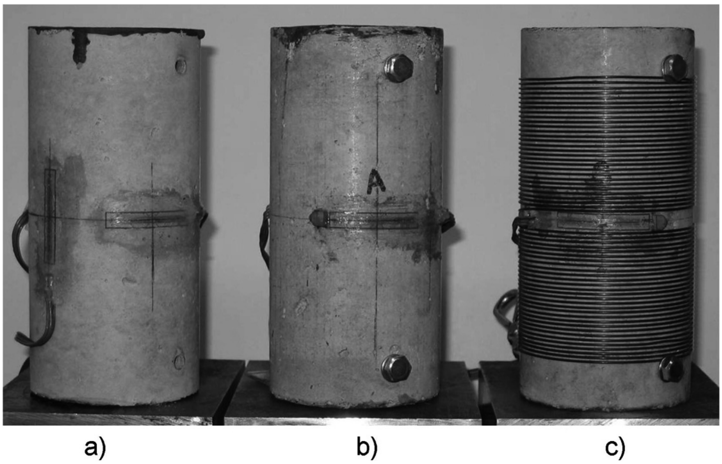

Fig. 2 Concrete cylinder types used in the study: (**a**) cylinder prepared for Young's modulus and Poisson's ratio determination (**b**) cylinder prepared for confinement strain measurements (**c**) same cylinder wrapped with a SMA wire with a 2 mm pitch

3.2 Specimen Preparation

Four cylinders were prepared from the same batch:

– One of them was aimed at measuring the mechanical properties of the concrete (Fig. 2a). It was equipped with two pairs of strain gauges. They were bonded onto the concrete surface at mid-height of the cylinder: two gauges were bonded opposite to each other parallel to its longitudinal axis; the other two were bonded opposite to each other along its mid-height circumference.
– The other three were prepared for the active confinement tests (Fig. 2b). Each cylinder was equipped with two strain gauges bonded opposite to each other along its mid-height circumference. The gauges were aimed at measuring the circumferential strain at the concrete surface of the cylinder in order to estimate the confinement stress induced in the concrete by the SMA wire during the test.

All gauges were 30 mm in length. According to the supplier specifications, the operational temperature is 80°C for the gauges and the connecting leads, 120°C for the adhesive.

In order to get a close to uniform confinement stress over the cylinder lateral surface, it was felt necessary to wrap the wire around the cylinder with a small constant pitch. Preliminary calculations showed that the choice of a 1 mm diameter wire with a constant 2 mm pitch would be a satisfying compromise. Owing to the cylinder dimensions, the total wire length required for wrapping one cylinder between the two thread inserts was about 19.9 m.

The preparation of each specimen consisted in a sequence of operations in order to prepare the SMA wire and to wrap it around the concrete cylinder under controlled temperature conditions:

– transforming the SMA wire in the self-accommodated martensite state – this was done by heating the wire up at a temperature over Af, then cooling it down at a temperature under Mf (Fig. 1c, steps 1 and 2);
– stretching the SMA wire at ambient temperature (under As) to obtain a specified prestrain in the reoriented martensite state (Fig. 1c, steps 4 and 5)
– wrapping the SMA wire around the concrete cylinder at ambient temperature (under As) with a constant pitch equal to 2 mm.

Practically, each SMA wire was coiled round a 350 mm diameter drum and kept in an oven at a temperature of 60°C for 30 min. Then, it was cooled down and kept in a freezer at a temperature of –30°C. After that, the wire was ready for stretching at ambient temperature. Despite its length (19.9 m), it was decided to stretch each wire as a whole in order to ensure a uniform prestrain. This was done by setting the wire horizontally and pulling its other end with a jack to a prescribed value. The vertical sag of the wire was taken into account for this operation. After stretching, the wire was wrapped around the concrete cylinder using a device specially designed to ensure a constant 2 mm pitch (Fig. 2c). All the operations were done at an ambient temperature between 18 and 21°C.

3.3 Thermal Loading and Strain Measurement

Thermal activation of the shape memory effect in the SMA wire was achieved by heating the wrapped cylinders at a temperature above Af (i.e. the $M \rightarrow A$ final transformation temperature).

For this purpose, the specimens were placed in an oven. The temperature was increased at a constant rate of 1.6°C/min up to 60°C, and then decreased to 23°C at a rate about –1.2°C/min. The total test duration was about 75 min. Values given by the circumferential strain gauges were monitored and recorded during the whole test for each cylinder.

The experiments were organized in two stages. In the former stage, the plain cylinders (i.e. without SMA wires) were tested under the conditions described above in order to record the influence of the thermal loading on the gauges and the concrete strains. In the later stage, the wrapped cylinders were tested under the same thermal conditions. For each specimen, the difference between the strain measurements obtained for the wrapped and the plain cylinder was assumed to reflect the net deformation of the concrete caused by the activation of the shape memory effect in the SMA, i.e. the net strains in the wrapped cylinder freed from the influence of temperature on the concrete and the gauge measurements.

4 Preliminary Tests

4.1 Determination of Concrete Characteristics

The mechanical characteristics required for the concrete in the present study are its Young's modulus E_c and its Poisson's ratio ν. For this purpose, compression tests were carried out 105 days after cast on the cylinder equipped with four strain gauges (Fig. 2a). The compressive stress was applied to the concrete in the range 0–2.5 MPa, which corresponds to the stress range expected in the wrapped cylinders during the confinement tests. Average values of the Young's modulus and the Poisson's ratio are calculated from the measured strains. The average values obtained are as follows: $E_c = 25.2$ GPa and $\nu = 0.193$.

4.2 Determination of SMA Wire Characteristics

The different steps described in Sect. 2 to create forces in SMAs were experimentally performed on a Ni-Ti wire coupon 150 mm in length. The aim was to determine the relationship between the tensile prestrain in the SMA wire in the martensite state and the tensile stress obtained in the wire after thermal activation of the shape recovery. Some points are here detailed:

– The ambient temperature was the same for all tests: 19 ± 1.5°C.
– The loading and unloading (steps 4 and 5) were applied with a MTS uniaxial testing machine. Tests differ in the stretching amplitude imposed to the wire at the end of step 4.

Figure 3 presents a typical strain-stress curve, corresponding here to the case 2 illustrated in Fig. 1d. Three quantities are defined:

– ε_{mar} is the strain obtained at the end of step 5, which is kept constant during the final thermal loading (steps 6 and 7),
– σ_{aus} is the maximum stress obtained in the austenite state (end of step 6),
– σ_{rec} is the residual stress so-called "recovery stress" at the end of the procedure.

Figure 4 presents the values obtained for σ_{aus} and σ_{rec} as a function of ε_{mar}. As predicted from Fig. 1d, the higher ε_{mar}, the higher σ_{aus}. It is also confirmed that high values of ε_{mar} lead to recovery stress values σ_{rec} lower than σ_{aus} (see case 2 in Fig. 1d). Indeed, σ_{rec} shows a constant value (205.3 MPa) for $\varepsilon_{mar} \geq 5.79 \cdot 10^{-3}$.

Finally, the Young's modulus of the austenite phase needs to be determined. To be sure that the tested wire coupon would be in the austenite state, it was first heated to a temperature higher than Af to obtain a purely austenite state. The return to room temperature did not produce martensite because the room temperature was higher than Ms. Then, the austenitic wire coupon was tensioned at ambient temperature. Finally, the Young's modulus of the SMA wire in the austenite state was determined by comparing the applied tensile stress with the longitudinal strain measured during the test. It was found to be equal to 62.9 GPa.

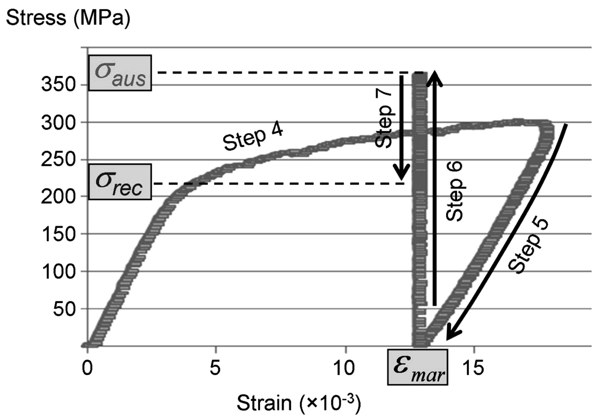

Fig. 3 Preliminary tests on Ni-Ti wires: typical strain-stress curve corresponding to the case 2 of Fig. 1d

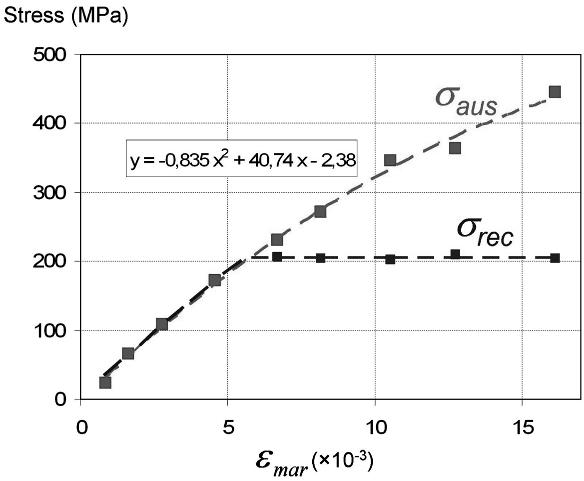

Fig. 4 Preliminary tests on Ni-Ti wires: results obtained as a function of ε_{mar} (see Fig. 3 for the meaning of ε_{mar}, σ_{aus} and σ_{rec})

5 Testing of Wrapped Cylinders

5.1 Characteristics of Tested Specimens

Two series of three specimens were prepared according to the procedure described in Sect. 3.2. The specimens are called C1 to C6, by order of increasing prestrain in the SMA wire. Data concerning the prestrain ε_{mar} and the corresponding recovery stresses σ_{aus} and σ_{rec} are listed in Table 1 for the six specimens. The letter (a) or (b) printed after every specimen name indicates which series the specimen belongs to.

Table 1 Effective prestrains (ε_{mar}) and recovery stresses (σ_{aus} at high temperature, σ_{rec} at ambient temperature) in the SMA wires for the tested specimens

	C1 (b)	C2 (a)	C3 (a)	C4 (b)	C5 (a)	C6 (b)
ε_{mar} (10^{-3})	2.08	3.76	4.95	6.22	8.84	10.71
σ_{aus} (N/mm^2)	78.8	139.1	178.9	218.9	292.4	338.2
σ_{rec} (N/mm^2)	78.8	139.1	178.9	205.3	205.3	205.3

5.2 Test Results

The cylinders were tested after ageing between 100 and 105 days after cast. All three specimens of the same series were placed together in the oven in order to achieve the prestressing by thermal activation of the memory shape effect in the SMA. As explained in Sect. 3.3, the net circumferential strains were obtained for each cylinder by correcting the values given by the gauges by the corresponding values previously recorded for the same cylinder previously tested without SMA wire (plain cylinder).

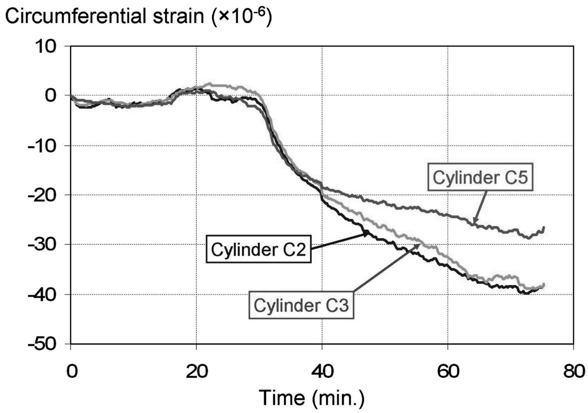

Fig. 5 Development of circumferential strains in cylinders C2, C3 and C5 (series a) during the thermal cycle

As an example, the net circumferential strains obtained for specimens C2, C3 and C5 (series a) are shown in Fig. 5. The competition between the shape recovery of the SMA wire due to the memory effect (transformation to austenite), and the thermal expansion in the wire and concrete materials results in small circumferential strains during the heating phase of the test, i.e. during the first 30 min of the thermal cycle. A change is observed when the temperature begins to decrease. The progressive development of a negative circumferential strain in the concrete observed in Fig. 5 shows the existence of a confinement effect caused by the developing recovery stress in the SMA wire. The strain evolution is pretty similar for the three samples, until the temperature reaches 50°C (i.e. 40 min after test beginning). Under 50°C, the circumferential concrete strains evolve separately in the three specimens. Finally, they stabilize when the temperature reaches about 23°C.

It can be observed that the final values of the circumferential strains are similar for specimens C2 and C3. A smaller strain value is obtained for specimen C5. This trend is in contradiction with the values expected for the recovery stress σ_{rec} in the three specimens (see Table 1): according to the respective prestrain $\varepsilon_{\mathrm{mar}}$ in the wire, the largest circumferential strain would be expected in specimen C5 and the smallest in specimen C2, with an intermediate value in specimen C3. The same trend is observed in series b (not presented here). This point will be discussed in Sect. 6.

5.3 Post-processing of Strain Gauge Measurements

Based on the hypothesis of isotropic plane state of stresses, the circumferential strain $\varepsilon_{\mathrm{c0}}$ caused by a uniform confinement stress σ_{cc} applied to a plain cylinder can be expressed as follows:

$$\varepsilon_{\mathrm{c0}} = (1 - \nu)\frac{\sigma_{\mathrm{cc}}}{E_{\mathrm{c}}}. \tag{1}$$

There is no SMA wire wrapped within the zone where the circumferential gauges are bonded to the concrete at the mid-height of the cylinder (see Fig. 2c). As a consequence, no confinement force is applied to the concrete, leading to lower concrete strains in this zone. Thus, the circumferential strain ε_{cc} to be expected at mid-height of a wrapped cylinder can be expressed as follows:

$$\varepsilon_{cc} = \frac{\varepsilon_{c0}}{\xi}, \tag{2}$$

where ξ is a correction coefficient ($\xi > 1$). A finite element analysis was carried out under the hypothesis of axi-symmetry in order to determine the appropriate value for ξ. Precise values were considered for the geometry and the mechanical characteristics of the wrapped cylinder. A value of 1.464 was obtained for the correction coefficient ξ.

From Eqs. (1) and (2), the confinement stress σ_{cc} corresponding to the circumferential concrete strain ε_{cc} measured at mid-height of a wrapped cylinder can be expressed as follows:

$$\sigma_{cc} = \xi \frac{E_c \varepsilon_{cc}}{(1 - \nu)}. \tag{3}$$

Based on local static equilibrium in the wrapped zone of the cylinder, the expression of the tensile force F in the SMA wire corresponding to the confinement stress can be easily derived:

$$F = \frac{pD}{2} \sigma_{cc}, \tag{4}$$

where p is the pitch and D is the diameter of the concrete cylinder.

The effective tensile stress σ_{SMA} in the SMA wire is obtained by dividing the force F by the cross-section area A_W of the SMA wire with account of Eq. (3), hence:

$$\sigma_{SMA} = \frac{\xi pD}{2(1 - \nu) A_W} E_c \varepsilon_{cc}. \tag{5}$$

Finally, the expected confinement stress $\sigma_{cc,exp}$ induced by the recovery stress σ_{rec} given in Table 1 for every tested specimen, is easily derived taking $F = A_W \sigma_{rec}$ in Eq. (4):

$$\sigma_{cc,exp} = \frac{2A_W}{pD} \sigma_{rec}. \tag{6}$$

Equations (3), (5) and (6) will allow us to derive the effective confinement stress σ_{cc} in the concrete and the effective tensile stress σ_{SMA} in the SMA wire from the values of the circumferential strain ε_{cc} measured during the thermal cycle, and to estimate the expected confinement stress $\sigma_{cc,exp}$ in terms of the expected recovery stress for each tested specimen.

5.4 Effective Confinement Stress

The values obtained for the net circumferential concrete strains ε_{cc} after thermal activation of the SMA memory effect and cooling down to 23°C are listed in Table 2 for the six tested specimens. The corresponding values of the confinement stresses σ_{cc} in the concrete are processed from the measured circumferential strain values ε_{cc} by means of Eq. (3). The expected values of the confinement stresses $\sigma_{cc,exp}$ are derived from Eq. (6) for the expected values of the recovery stress σ_{rec} given in Table 1. In order to compare the expected values with the effective values of the confinement stress derived from tests, the $\sigma_{cc}/\sigma_{cc,exp}$ ratio was calculated and is plotted in Fig. 6 in terms of the initial prestrain ε_{mar} in the SMA wire.

Surprisingly, the confinement effect is much higher than expected ($\sigma_{cc}/\sigma_{cc,exp} > 1$) when the initial prestrain is low. On the contrary, the confinement effect is much lower than expected ($\sigma_{cc}/\sigma_{cc,exp} < 1$) when the prestrain in the SMA wire is high. In between, the $\sigma_{cc}/\sigma_{cc,exp}$ ratio sharply decreases when the SMA prestrain is

Table 2 Results for the tested specimens

	C1 (b)	C2 (a)	C3 (a)	C4 (b)	C5 (a)	C6 (b)
ε_{cc} (10^{-6})	–39.4	–39.8	–39.0	–41.7	–28.6	–24.9
σ_{cc} (N/mm^2)	–1.80	–1.82	–1.78	–1.91	–1.31	–1.14
$\sigma_{cc,exp}$ (N/mm^2)	–0.83	–1.47	–1.89	–2.17	–2.17	–2.17
σ_{SMA} (N/mm^2)	170.6	172.4	168.9	180.6	123.9	107.8
$\sigma_{cc}/\sigma_{cc,exp}$ (–)	2.16	1.24	0.94	0.88	0.60	0.53

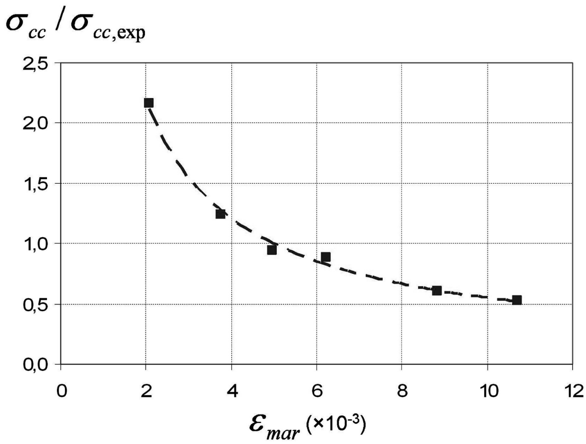

Fig. 6 Effective to expected confinement stresses ratio in terms of the wire prestrain

increased. The balance ($\sigma_{cc}/\sigma_{cc,exp} = 1$) is obtained for prestrain in the wire of about $5{\cdot}10^{-3}$. This result highlights the complex interaction between cylinder and wire responses. It can be concluded that the confinement effect in the cylinder is not resulting only from the recovery of the tensile prestrain in the wire. An additional phenomenon should be considered involving a more complex interaction between the SMA wire and the concrete cylinder. In the next section, the hypothesis of an influence of the curvature caused by the wrapping of the wire around the cylinder is investigated.

6 Effect of the Curvature on the Recovery Stress

It is obvious that the effective tensile stresses σ_{SMA} obtained in the wrapped SMA wires (see Table 2) are in no agreement with the recovery stresses σ_{rec} expected from the prestrains ε_{mar} produced by stretching of the martensitic wires before wrapping (Table 1). The two sets of values are plotted in Fig. 7 in terms of ε_{mar}. On the left hand side of the figure ('low' ε_{mar} values), the effective tensile stress σ_{SMA} has a constant value, whereas the expected values σ_{rec} increase with increasing values of ε_{mar}. On the right hand side of the figure ('high' ε_{mar} values), the effective tensile stress σ_{SMA} decreases, with a maximum 'loss' about 37%.

Based on these observations, the issue of an additional interaction phenomenon, due to the effect of the wrapping of the wire on the cylinder can be addressed. As a matter of fact, the wrapping induces an additional deformation of the wire in order to fit the geometry of the cylinder. Indeed, the additional deformation corresponds

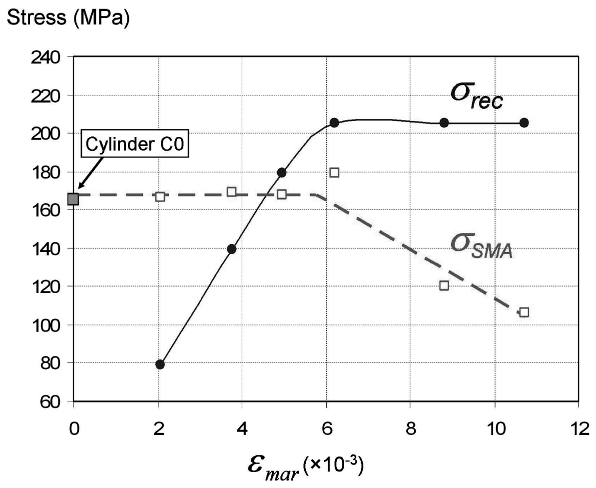

Fig. 7 Comparison between the expected recovery stress and the effective residual stress in the wire in terms of the wire prestrain

to a bending curvature with a fixed value. Taking the cylinder and the wire radii into account, the curvature is found equal to 26.5 m^{-1}. The corresponding maximum strain in the martensitic wire is equal to the curvature multiplied by the wire radius. It is found equal to 13.3 10^{-3}, which is higher than the highest value of the prestrain ε_{mar} in the martensitic wire (see Table 1). For low ε_{mar} values, the resulting strains in the martensitic wire are dominated by the curvature effect, leading to about constant effective stresses in the austenitic wire after the thermal cycle. For high ε_{mar} values, the strains and stresses induced by the curvature combine with the tensile prestrains, leading to decreasing effective stresses in the SMA wire. The fact that the effective values of the wire stresses are lower than the maximum value (205.3 MPa) obtained for the recovery stress can be a result of the gradient in the additional strain through the wire diameter.

Finally, in order to confirm the influence of the wire curvature on the confinement effect, one additional test was carried out with a cylinder wrapped with a non-stretched martensitic wire, i.e. $\varepsilon_{mar} = 0$ and $\sigma_{rec} = 0$. The final effective confinement stress obtained in the concrete was found equal to 1.77 MPa, which is pretty close to the values obtained for specimens C1 to C3 (see Table 2). The effective stress in the SMA wire was found equal to 167.6 MPa. This value is plotted in Fig. 7 (cylinder C0). It can be concluded that the confinement effect is significantly modified by the curvature strains due to the wrapping of the SMA wire on the cylinder.

7 Conclusion

The confinement of concrete cylinders wrapped with Ni-Ti SMA wires was investigated. The main results are as follows:

1. An active confinement at ambient temperature is possible using a SMA wire with suitable transformation temperatures. The martensite start (Ms) and the austenite start (As) temperatures must be chosen to be lower and higher respectively than the ambient temperature. So it is possible to stretch the wires in their martensitic state before wrapping around the cylinders. The recovery forces are developed by heating and they are retained when returning to ambient temperature.
2. The influence of the initial stretch of the wires on the final confinement is evidenced. Surprisingly, it is observed that the confinement level is constant for low-stretched wires and decrease for higher values of wire stretch. This behaviour is not predictable from results obtained with straight wire coupons tested under uniaxial tension.
3. A complex interaction between cylinder and wire responses may explain this result. An additional test with a non-previously stretched wire shows that an active confinement is also obtained. This result illustrates that the curvature due to the wrapping around the cylinders has an effect on the confinement.

References

1. G. Pijaudier-Cabot, J.-M. Reynouard, J.-M. Torrenti, *Mechanical Behavior of Concrete* (ISTE & Wiley, London, 2010)
2. K. Otsuka, C.M. Wayman, Shape Memory Materials (Cambridge University Press, Cambridge, 1999)
3. S. El-Tawil, J. Ortega-Rosales, Prestressing concrete using shape memory alloy tendons. ACI Struct. J. **101**, 846–851 (2004)
4. Z. Deng, Q. Li, H. Sun, Behavior of concrete beam with embedded shape memory alloy wires. Eng. Struct. **28**, 1691–1697 (2006)
5. H. Li, Z. Liu, J. Ou, Behavior of a simple concrete beam driven by shape memory alloy wires. Smart Mater. Struct. **15**, 1039–1046 (2006)
6. P. Soroushian, K. Ostawari, A. Nossoni, H. Chowdhury, Repair and strengthening of concrete structures through application of corrective posttensionning forces with shape memory alloys. Transp. Res. Rec. **1770**, 20–26 (2001)
7. M. Motavalli, C. Czaderski, A. Bergamini, L. Janke, Shape Memory Alloys for Civil Engineering Structures – On the Way from Vision to Reality. AMCM'2008 Lodz, Poland, pp. 91–108
8. L. Janke, C. Czaderski, M. Motavalli, J. Ruth, Applications of shape memory alloys in civil engineering structures: overviews, limits and new ideas. Mater. Struct. **38**, 578–592 (2005)
9. E. Choi, Y.S. Chung, B.S. Cho, T.H. Nam, Confining concrete cylinders using shape memory alloy wires. Eur. Phys. J. **158**, 255–259 (2008)
10. N. Krstulovic-Opara, P.D. Thiedeman, Active confinement of concrete members with self-stressing composites. ACI Mater. J. **97**, 297–308 (2000)
11. N. Krstulovic-Opara, A.E. Naaman, Self-stressing fiber composites. ACI Struct. J. **97**, 335–345 (2000)
12. K. Moser, A. Bergamini, R. Christen, C. Czaderski, Feasibility of concrete prestressed by shape memory alloy short fibers. Mater. Struct. **38**, 593–600 (2005)
13. K. Bhattacharya, Microstructure of Martensite: Why It Forms and How It Gives Rise to the Shape-Memory Effect (Oxford University Press, Oxford, 2003)
14. P.H. Lin, H. Tobushi, K. Tanaka, C. Lexcellent, A. Akai, Recovery stress of TiNi shape memory alloy under constant strain. Arch. Mech. **47**, 281–293 (1995)

http://www.springer.com/978-3-642-12666-6

Materials with Complex Behaviour
Modelling, Simulation, Testing, and Applications
da Silva, L.F.M.; Altenbach, H. (Eds.)
2010, XII, 372 p. 268 illus., Hardcover
ISBN: 978-3-642-12666-6